HHS Public Access

Author manuscript

Circ Res. Author manuscript; available in PMC 2016 November 06.

Published in final edited form as:

Circ Res. 2015 November 6; 117(11): e80–e89. doi:10.1161/CIRCRESAHA.115.307207.

Prevention of Abdominal Aortic Aneurysm Progression by Targeted Inhibition of Matrix Metalloproteinase Activity with Batimastat-Loaded Nanoparticles

Nasim Nosoudi[1], **Pranjal Nahar-Gohad**[1], **Aditi Sinha**[1,2], **Aniqa Chowdhury**[1], **Dr Patrick Gerard**[1], **Christopher G. Carsten**[3], **Bruce H. Gray**[3], and **Naren R. Vyavahare**[1]

[1]Department of Bioengineering, Clemson University, Clemson, SC 29634, USA

[2]Edwards Lifesciences Center for Advanced Cardiovascular Technology, University of California, Irvine, CA 92697, USA

[3]Division of Vascular Surgery, Greenville Health System, Greenville, SC

Abstract

Rationale—Matrix metalloproteinases (MMPs)-mediated extracellular matrix destruction is the major cause of development and progression of abdominal aortic aneurysms (AAA). Systemic treatments of MMP inhibitors have shown effectiveness in animal models but it did not translate to clinical success either due low doses used or systemic side-effects of MMP inhibitors. We propose a targeted nanoparticle based delivery of MMP inhibitor at very low doses to the AAA site. Such therapy will be an attractive option for preventing expansion of aneurysms in patients without systemic side effects.

Objective—Our previous study showed that poly D, L-lactide (PLA) nanoparticles (NPs) conjugated with an anti-elastin antibody could be targeted to the site of an aneurysm in a rat model of AAA. In the study reported here, we tested whether such targeted NPs could deliver the MMP inhibitor batimastat (BB-94) to the site of an aneurysm and prevent aneurysmal growth.

Methods and Results—PLA NPs were loaded with BB-94 and conjugated with an elastin antibody. Intravenous injections of elastin antibody-conjugated BB-94-loaded NPs (EL-NP-BB94) targeted the site of aneurysms and delivered BB-94 in a calcium chloride injury-induced AAA in rats. Such targeted delivery inhibited MMP activity, elastin degradation, calcification, and aneurysmal development in the aorta (269% expansion in control vs. 40% EL-NP-BB94) at a low dose of BB-94. The systemic administration of BB-94 alone at the same dose was ineffective in producing MMP inhibition.

Conclusions—Targeted delivery of MMP inhibitors using NPs may be an attractive strategy to inhibit aneurysmal progression.

Address correspondence to: Dr. Naren R. Vyavahare, Professor and Hunter Endowed Chair, Department of Bioengineering, Clemson University, Clemson, SC 29634, Tel: (864) 656-5558, Fax: (864) 656-4466, narenv@clemson.edu.

DISCLOSURES

None.

Subject terms

Animal models of human disease; Pharmacology; Treatment; Aneurysm Abdominal aortic aneurysm; MMP inhibitors; nanoparticle; targeted therapy; batimastat; vascular remodeling; drug delivery system; cardiovascular disease

INTRODUCTION

Abdominal aortic aneurysm (AAA) characterized by dilation of the abdominal aorta is one of the top-10 causes of death among older men.[1] Although the cause of AAA remains unknown in the majority of cases, several key regulators of AAA pathogenesis are known. Matrix metalloproteinases (MMPs) have been shown to play a major role in progressive extracellular matrix (ECM) degradation in AAA.[2, 3] Under inflammatory conditions, infiltrating macrophages, vascular smooth muscle cells, endothelial cells, and adventitial fibroblasts secrete pro-MMPs; cleavage of the pro-MMP subunit activates the MMPs, causing ECM degradation. MMP activity may be naturally suppressed by tissue inhibitors of matrix metalloproteinases (TIMPs), which comprise a family of four protease inhibitors: TIMP1, TIMP2, TIMP3, and TIMP4.[4] An improper balance between MMPs and TIMPs shifts equilibrium towards matrix degradation in several vascular conditions, such as AAA, atherosclerosis, hypertension, and calcification.[5]

Several types of MMPs are expressed in AAA tissue, including MMP-1, MMP-2, MMP-3, MMP-9, and MMP-12.[6] MMP-9 and MMP-2 knockout mice do not develop aneurysms, suggesting that these MMPs play a major role in development of AAA.[7] A number of synthetic MMP inhibitors (e.g., doxycycline- and hydroxamate-based) are known to decrease MMP activity[8] and prevent medial destruction.[9] Synthetic MMP inhibitors with a hydroxamate (-CONHOH) group bind zinc atoms and suppress MMP enzymes.[10] Among the many hydroxamate-based MMP inhibitors are marimastat, solimastat, prinomastat, cipemastat, and batimastat (BB-94).[11, 12] It has been shown that BB-94 was one of the first synthetic MMP inhibitors to be tested clinically to reduce MMPs in cancers with advanced malignancies.[13] However, its effectiveness is limited by its poor water solubility when administered orally, requiring parenteral administration. In several studies, systemic administration of MMP inhibitors effectively reduced aneurysmal onset in animal models[12, 14, 15], but systemic delivery can cause off-target inhibition of the MMP activities essential for normal homeostasis.[16] Although there are no in vivo studies of targeted delivery of MMP inhibitors to the aneurysmal site, a recent in vitro study showed the potential of delivering doxycycline-loaded nanoparticles (NPs) for localized elastic matrix stabilization and regenerative repair in AAA.[17] Doxycline was also shown to reduce mRNA stability for MMP-2 and inhibit MMP activity that way.[18]

In this study, we tested the hypothesis that systemic delivery of elastin-antibody conjugated NPs loaded with BB-94 would be targeted specifically to the aneurysm site, would slowly release the drug there, and would inhibit local MMP activity and subsequent aneurysm expansion. Such targeted MMP inhibition would require smaller and less frequent drug doses than systemic administration, and thus systemic side effects would be minimized.

METHODS

Synthesis of batimastat-loaded nanoparticles (EL-NP-BB94)

Poly (D,L-lactide) (PLA) NPs were prepared using the solvent-diffusion-based nano-precipitation method.[19] (Supplementary data).

Nanoparticle yield

The total final dry weight of the NPs was recorded, and NP yield was calculated using the formula shown below:

$$\mathrm{NPyield}\% = \frac{\mathrm{Final\ \ dry\ \ weight}}{\mathrm{Initial\ \ weight}} \times 100$$

Nanoparticle characterization

Particle size, ζ-potential and transmission electron microscopy (TEM) were performed to characterize the NPs. (Details are in Supplementary data).

Nanoparticle degradation studies

Blank NPs were suspended in phosphate buffered saline (PBS) and stirred at 37°C to test polymer degradation. NP degradation was monitored by measuring the weight of the remaining NPs at different time points (1, 7, 14, 21, and 28 days) after lyophilization. The percent weight loss was calculated using the difference in the remaining dry weight and the initial weight. We also tested blank NPs degradation by gel permeation chromatography (GPC). (Details are in Supplementary data).

Loading efficiency and release profile of BB-94

Loading efficiency was calculated by dissolving NPs in Dimethyl sulfoxide, determining BB-94 concentration at λ (max) = 285 nm using UV spectrophotometry, and using the equation shown below:

$$\%\mathrm{Loading} = (\mathrm{BB-94weight/total\ \ weight\ \ ofNPs}) \times 100$$

Percent release was calculated as:

$$\%BB\text{-}94Released = \frac{(\mathrm{Initially\ \ loadedBB} - 94) - (\mathrm{ResidualBB} - 94)}{\mathrm{Initially\ \ loadedBB} - 94} \times 100$$

(Details are in Supplementary data).

Conjugation of elastin antibody to NPs

Traut's reagent (34 μg, G-Biosciences, Saint Louis, MO) was used for thiolation of 10 μg of rabbit anti-rat elastin antibody (United States Biological, Swampscott, MA), and the mixture was incubated in HEPES buffer (20 mM, pH=9.0) for an hour at room temperature.

Thiolated antibodies were rinsed with HEPES buffer and added to the NPs (4 μg antibody per 1 mg NPs) and then incubated overnight for conjugation. After incubation, antibody-conjugated NPs were washed twice with PBS, centrifuged (10000 rpm for 10 minutes), and suspended in 0.3% rat serum albumin for an in vivo animal study.[19]

BB-94 activity

To test if the BB-94 loaded in the NPs was still in active form, sodium dodecyl sulfate-polyacrylamide gel electrophoresis (SDS-PAGE) zymography was performed.[20] (Details are in Supplementary data).

Reverse zymography for TIMP activity

Equal amounts of protein from RASMC-conditioned cell culture media (BB-94 treated or control) were loaded in 15% reverse zymogram gel containing 1.5% gelatin and collagenase (20 units) under nondenaturing and nonreducing conditions.[20] (Details are in Supplementary data).

NP toxicity for rat aortic smooth muscle cells (RASMCs) and rat aortic endothelial cells (RAOEC)

A standard MTT assay was performed to measure the cytotoxicity of NPs to RASMCs and RAOECs. (Details are in Supplementary data).

Nanoparticle uptake by macrophages

Elastin-antibody conjugated NPs were loaded with fluorescent dye, 1, 1-dioctadecyl-3, 3, 3, 3-tetramethylindotricarbocyanine iodide (DIR), as described previously[19]. Macrophages (RAW 264.7, ATCC® TIB-71™) were grown in 24-well tissue culture plates followed by incubation with EL-DIR-NPs (1 mg/ml) at 37°C in 5% CO_2 for 4 hours and 24 hours. Cells were washed three times with sterile PBS and imaged before and after washing using EVOS® XL Cell Imaging System to determine NP uptake. As controls for charge and size, we prepared two different batches of NPs, one with positive surface charge and one with smaller-sizeNPs. To create a positive surface charge, NPs were coated with chitosan[21] (molecular weight 600K-800K) (ACROS, NJ). To study cytotoxicity, rat bone marrow macrophage cells (Cell Biologics, Inc., RA-6030F) were grown in 24-well tissue culture plates followed by incubation with blank and BB94 -NPs (0.5, 1, 2 mg/ml). A standard Live /Dead assay was performed after 24 hours.

Feasibility of nanoparticle targeting in vivo

Local elastin damage in the rat abdominal aortic region was induced by perivascular application of calcium chloride.[22] Briefly, 19 male Sprague-Dawley (SD) rats (5–6 weeks old) were placed under general anesthesia (2% to 3% isoflurane). The infrarenal abdominal aorta was exposed and treated periadventitially by placing 0.50 mol/L $CaCl_2$-soaked sterile cotton gauze on the aorta for 15 minutes. The treated area was flushed with warm saline, and the abdominal incision was closed with sutures. Animals were allowed to recover and given a normal diet for ten days. Adventitial inflammation and elastic lamina degradation has previously been shown to occur within ten days in this model. After ten days, rats were

divided into two groups and put through treatment with batimastat-loaded NPs or blank NPs. NPs loaded with BB-94 and conjugated with elastin antibody (named EL-NP-BB94 hereafter) at ~10 mg/kg body wt. were suspended in 200 μl of 0.3% rat serum albumin (Sigma Aldrich, St. Louis, MO) and were injected through the tail vein (n=5). Control animals received elastin antibody-conjugated blank NPs (named EL-NP-Blank hereafter) (n=5). Three additional rats were injected with elastin antibody conjugated and DIR dye-loaded NPs (named EL-NP-DIR hereafter) to monitor delivery of the NPs by in vivo imaging. As a negative control, IgG antibody-conjugated NPs loaded with DIR dye (named IgG-NP-DIR hereafter) were injected through the tail vein (n=3). To study if the systemic delivery of low-dose BB-94 affects MMP activity in the aorta, three rats received the same amount of BB-94 (600 μg of BB-94 /kg body wt.) dissolved in 200 μL PBS solution with 0.01% Tween 20 (Merck, Germany) by intraperitoneal injection.

Two days (48 h) after treatment, the rats were euthanized, and thoracic and abdominal aortic tissue segments were explanted and snap-frozen in liquid nitrogen. Total protein from the aortic samples was extracted by pulverizing liquid nitrogen-frozen tissue samples and homogenizing them in RIPA extraction buffer (50 mM Tris-HCl pH 7.4, 150 mM NaCl, 1 mM EDTA, 1% Triton X-100, 1% Sodium deoxycholate, 0.1% SDS, with protease inhibitor cocktail) (Roche Diagnostic GmbH, Germany) according to the manufacturer's protocol. Sections of thoracic and abdominal aortic tissue were embedded in Optimal Cutting Temperature compound (OCT) for cryostat sectioning. For DIR-loaded NP groups, whole fresh aortas and all organs were harvested and imaged using Caliper IVIS Lumina XR (Hopkinton, MA) with Ex/Em of 745/795 nm for studying targeting and biodistribution of NPs.

MMP activity in rat aorta

The total protein from the harvested aortic tissue after 48 hours of treatment was quantified using the BCA Protein Assay Kit (Pierce, IL). An internally quenched peptide substrate that is specific to MMP-2 and 9 (excitation 280 nm, emission 360 nm, MMP Substrate III, Anaspec, CA) was used to measure MMP activity. One mg of substrate dissolved in 50 μl Dimethyl sulfoxide was diluted in 10 ml of development buffer (50 mM Tris Base, 5 mM $CaCl_2 \cdot 2H_2O$, 200 mM NaCl, 0.02% brij 35). Development buffer (96 μl) was mixed with 2 μl of the extracted protein along with 2 μl of substrate stock solution and incubated for one hour at 37°C. Endpoint florescence intensity was read using a fluorescence plate reader.

Nanoparticle targeting to inhibit aneurysm progression

To study long-term aneurysmal inhibition, another set of 13 rats was used. AAAs were induced by perivascular application of calcium chloride[22] as shown above. Ten days after injury, NPs (~10mg/kg body wt.) were injected via tail vein once a week for four weeks (n=5 EL-NP-BB94, n=5 EL-NP-Blank, and n=3 EL-NP-DIR). Rats were euthanized on day 38, and organs and aortae were harvested. IVIS imaging was used to confirm targeting and bio distribution in the EL-NP-DIR group. Aortic tissues from the EL-NP-Blank and EL-NP-BB94 groups were harvested as described above.

In situ zymography

To examine activity of MMPs in the aortic tissue samples in situ, zymography was performed on histological sections of aortae isolated at 48 hours and 38 days after NP injection. Gelatinolytic activity was demonstrated in unfixed cryostat sections (8 μm thick) using DQ-gelatin as a substrate (Life, IL). Cryostat sections of abdominal aorta were air-dried for 10 minutes. One part DQ-gelatin (1 mg/ml of DI water) was mixed with nine parts 1% agarose (Promega, WI) in PBS containing DAPI (1 μg/ml) (Life Technologies, IL). A drop of the mixture was added to each section; these were then incubated in development buffer for one hour at 37° C. As a positive control, in one sample MMP activity was blocked by MMP inhibitor 1, 10-phenanthroline monohydrate (0.2mmol/L) (Life Technologies, OR). Images were captured using EVOS® XL cell imaging system.

Histological analysis

Formalin-fixed samples were embedded in paraffin, and 5 μm sections were mounted on glass slides and heated overnight to adhere the tissues to the slides and melt the paraffin. Subsequently, the slides were deparaffinized with xylenes and graded ethanol and stained with hematoxylin and eosin for tissue morphology, Verhoeff-van Gieson (VVG) for elastic fibers, and Alizarin Red S with a Light Green SF counterstain for calcification.

Immunostaining for macrophages (CD80)

Aortic sections from the 38-day aneurysm study were used. Tissues preserved with formalin were embedded in paraffin and sectioned as previously described. Subsequently, the slides were deparaffinized with xylenes and graded ethanol, and antigen retrieval was done using the HCl method. The slides were incubated overnight at room temperature with the primary antibody, Mouse Anti Rat CD80 (Bio-Rad, Hercules, CA). Subsequently, the slides were incubated for 1 hour with the secondary antibody, Cy7 goat anti-mouse IgG (H+L) (Bioss Inc., MA), and DAPI nucleic acid stain and then imaged with a fluorescent microscope, EVOS ® XL Cell Imaging System.

Aneurysmal development

Initial external diameter was measured at the time of the calcium chloride ($CaCl_2$) application. Final aortic diameter was recorded before euthanasia on Day 38. Aneurysmal development was calculated as shown below:

$$\text{aneurysmal development}\% = \frac{Final\ external\ diameter - Initial\ external\ diameter}{Initial\ external\ diameter} \times 100\%$$

Statistical analysis

In vitro experiments were performed in triplicate and repeated twice; for in vivo studies, five animals were used per group per time point. Student's t test was performed using Microsoft Excel, and exact permutation test was performed using the NPAR1WAY procedure in SAS. The data are expressed as the mean ± standard deviation; results were considered to be significant when P-values ≤0.05.

RESULTS

Nanoparticle characterization

NPs were prepared with three different initial BB-94 concentrations (5:1, 10:1, 15:1 polymer-to-drug ratio). No significant differences were found for the percent yield of NPs among the three batches. Increasing the initial BB-94 concentration during NP preparation did not increase the final BB-94 loading in the NPs. Particle-surface charge was dependent on initial polymer to BB-94 ratios. All BB-94-loaded NPs were negatively charged; however, a higher polymer to BB-94 ratio led to a more-negative surface charge (Table 1).

NP degradation and BB-94-release study

A higher polymer-to-BB-94 ratio led to a smaller NP size, which was confirmed visually by TEM (Fig 1A). When suspended in DI water, Blank-NPs lost substantial weight (65±4.5%) in four weeks; the majority of weight loss occurred in the first week (45.65±6.8) (Fig 1B). This data was corroborated by NP degradation seen in the GPC study (Supplementary data).

In vitro BB-94 release from the NPs was gradual and continued up to eight days. Although final BB-94 loading was similar for all polymer-to-BB-94 ratios, the BB-94 release profile varied with the starting BB-94 concentration (Fig 1C). Slower release was observed in NPs with a 5:1 polymer-to-BB-94 ratio, while significant burst release was observed when the initial BB-94 concentration was lower (10:1 or 15:1 polymer: BB-94 ratio). BB-94 release was more controlled for the batch with a higher starting BB-94 concentration (5:1 polymer: BB-94 ratio), so these NPs were chosen for further study.

Activity of BB-94

The activity of the BB-94 loaded in NPs was examined using gel zymography. When extracted BB-94 was added to the development buffer, pro-MMP-2 (72 kDa), active MMP-2 (62kD), and MMP-9 (92 kDa) activities were inhibited completely (Fig 2A). When BB-94 extracted from the NPs was added to the RASMC cultures, ninety percent of MMP-9 (92 kDa) and ten percent of MMP-2 (62 kDa) activity were inhibited (Fig 2B). Notably, more MMP-2 remained in the pro-form (inactivated, 72kD) when BB-94 was added to cell cultures (Fig 2B). There was no significant difference in the expression of tissue inhibitors of metalloproteinase-2 (TIMP-2) (21 kDa) between control and BB-94-treated cells (Fig 2C). These results suggest that BB-94 loaded NPs inhibited MMPs without affecting TIMP-2 levels.

NP cytotoxicity and cellular uptake

RAOEC and RASMC viability showed no significant change in 24 hours in the presence of NPs when compared to the control (Fig 3 A & Fig 3B). We have already shown that such NPs are not taken up by VSMCs.[19] Inflammatory cells such as macrophages are commonly present at the site of AAA. Thus, we determined whether our NPs were resistant to macrophage uptake. NPs labelled with a DIR dye were incubated with macrophage cell cultures for 24 hours (ζ-potential: −29.1±5.1, size: 196.28±3.2 nm). Due to the negatively charged surface of the chosen NPs, no macrophage uptake was observed (Fig 3C–a_1,a_2,a_3). When the surface-charge was changed to positive with the addition of chitosan, (ζ-potential:

+20.28±4.93), NPs could be seen in the cell cytoplasm; this suggests that they were taken up by macrophages (Fig 3C-b_1,b_2,b_3). When NP size was changed to ~125 nm and the surface charge remained negative (ζ-potential: −83 ±2.8), there was again significant uptake by macrophages (Fig 3C-c_1,c_2,c_3). Overall, ~200 nm NPs with negative surface charge that were chosen for further studies were resistant to macrophage uptake. Bone marrow macrophage viability showed no significant change in 24 hours for blank and BB-94 loaded NPs at the thirteen fold concentration used in vivo (Fig 3D).

In vivo NP targeting and MMP inhibition

We have shown that NPs with a surface conjugated anti-elastin antibody can target the site of aortic injury in this animal model.[19] We confirmed in vivo targeting, by observing localized fluorescence at the injury site of the abdominal aorta for the EL-NP-DIR group, this suggests excellent targeting to the injured aorta (Fig 4A), while no fluorescence was observed in the injured aorta for control IgG-NP-DIR group (Fig 4A).

We next examined whether NPs loaded with BB-94 would target the injury site and inhibit local MMP activity. When normalized to total protein content fluorescence intensity data showed that the abdominal aorta had ~50% higher MMP activity than the thoracic aorta in the EL-NP-Blank group (Fig 4B). This result suggests that MMPs were activated by $CaCl_2$-mediated injury and that blank NPs targeted to the abdominal aorta did not suppress MMP activity. The EL-NP-BB94 group showed 56% lower MMP activity in the abdominal aorta in comparison to the thoracic aorta, suggesting that MMP activity was completely suppressed at the injury site (Fig 4B). When the same concentration of BB-94 was delivered systemically by intraperitoneal injection (IP), it was ineffective in suppressing local MMP activity in the abdominal aorta (Fig 4B). These results were further confirmed by *in situ* zymography studies on histological sections of abdominal aorta in different groups. The green fluorescence in this assay is caused by the enzymatic degradation of DQ gelatin, which directly corresponds to the MMP activity in the sections. Intense green fluorescence corresponding to higher MMP activity was found in the sections of the abdominal aortae in the control animals receiving EL-NP-Blank or IP injected BB-94 (IP-BB-94); a significant suppression of MMP activity was observed in the BB-94 NP group (EL-NP-BB94), (Fig 4C). This was similar to the positive controls, where MMP activity was inhibited by the addition of 1, 10-Phenanthroline during *in situ* zymography.

Long-term targeting and biodistribution of NPs

With encouraging results in the 48-hour targeting experiment, we next determined if such targeting could inhibit MMP activity and aneurysmal development for prolonged periods. Because our BB-94-release study showed slow release for up to seven days, we decided to inject elastin-antibody conjugated NPs once weekly for four weeks. After injections (4 injections over a total of 38 days after the first $CaCl_2$ injury), a three-fold increase (from 26.3 to 78.7%) was seen in the fluorescence signal in the abdominal aorta for the EL-NP-DIR group as compared to a single injection (Fig 5A compared to Fig 4A), indicating more NPs accumulated at the injury site. Bio distribution of NPs (Fig 5B) showed NPs in lung, liver, kidneys, and spleen in addition to the aorta at 48 hrs after injection. After 38 days and 4 weekly injections, the signal decreased from 0.78 to 0.003% for the kidneys, from 15 to

2.7% for the liver, and from 48 to 18% for the spleen in comparison to the 2-day study (Fig 5B). These data show that additional NPs accumulated at the injury site, while other organs were clearing non-targeted NPs. More importantly, the NPs were seen infiltrating from the adventitial side of the aneurysmal aorta through the vasa vasorum rather than from the luminal side and then attaching to the degraded elastic lamina deep within the medial layer (Fig 5C).

Long-term inhibition of MMPs and aneurysmal development

When NPs were injected weekly for four weeks after $CaCl_2$ injury, MMP activity was still suppressed in animals receiving EL-NP-BB94 NPs (similar to the 48-hour study), while MMPs remained elevated in the EL-NP-Blank group (Fig 5D).

Hematoxylin and eosin staining showed significant inflammation in the adventitia in the EL-NP-Blank group, while the EL-NP-BB94 group maintained greater structural integrity and had little inflammation (Fig 6A and Fig 6E respectively). Verhoeff-van Gieson (VVG) staining revealed the elastic lamina was broken and damaged in the EL-NP-Blank group, but elastin preservation was observed in the EL-NP-BB94 group (Fig 6B and Fig 6F). Similarly, alizarin red S staining showed heavy medial calcification in the (EL-NP-Blank) group and a substantial reduction in calcification in the BB94-treated group (EL-NP-BB94) (Fig 6C and Fig 6G). Macrophage immunohistochemistry revealed that the blank NP group had a higher density of M1 macrophages in the adventitia and ruptured media in comparison to the BB-94 group (Fig 6D and Fig 6H).

We next determined aneurysmal expansion by measuring the external-aortic diameter (Fig 7 A and Fig 7B). When control blank NPs were injected (EL-NP-Blank), a large increase in diameter compared to the size before injury was observed (269.5±56%), suggesting that targeted blank NPs did not inhibit aneurysmal development. However, when BB-94-loaded NPs were injected, significant suppression of aneurysms was observed (40.25±26% increase in diameter) (Fig 7).

DISCUSSION

This study demonstrates that the use of targeted NPs carrying a potent MMP inhibitor can successfully inhibit local MMP activity in inflammatory vascular conditions such as AAA. We optimized NP size, surface charge, and BB-94 loading. Our data agree with the literature: During NP preparation, the particle size increased with increasing drug concentration and the negative surface charge decreased.[23] Particle size and drug loading are important parameters that dictate the release of a drug from NPs. The negative surface charge facilitates electric repulsion among NPs, thus increasing NP stability.[24] Surprisingly, increasing initial BB-94 concentration did not lead to a higher amount of BB-94-loading; the maximal loading was only 6–8% of BB-94 in PLA. This may have occurred because of the physical properties of the original drug.[25] Although drug-loading was similar, drug dispersion within NPs, and thus ultimate release, varied with initial drug concentration. Our study shows that higher polymer content (15:1 and 10:1 polymer to BB-94 ratio) resulted in burst release on day 1. This may have occurred due to the smaller particle size with higher surface area for drug diffusion. NPs in the 5:1 polymer-to-BB-94-ratio batch had the biggest

particle size and showed a more-controlled release because of either lower surface area or better drug encapsulation. Our NP degradation data with blank NPs showed significant weight loss after 7 days and an increase in polymer degradation products as assessed by GPC (supplementary data), suggesting that drug diffusion and polymer degradation occurred simultaneously.

Maintaining drug activity during NP synthesis is necessary for success in targeting. We showed that BB-94 extracted from NPs suppressd MMP activity both in gel zymography and in cell cultures. We found that adding BB-94 to the development buffer during gel zymography was more effective in inhibiting MMPs (both the active and pro forms) than adding to cell culture media. It is possible that BB-94 dissociated during gel electrophoresis when the cell culture media was loaded in gels and, thus caused lower MMP inhibition. The findings from reverse zymography showed no significant difference in the expression of TIMP-2 protein within the groups; this is consistent with the literature showing that BB-94 has no effect on TIMPs.[26]

Particle size and charge are important criteria in targeting NPs to the vasculature. It has been shown that NP-targeting of vascular ECM in an aneurysmal site occurred for particle sizes below 200 nm.[19] That study also showed that a negatively charged NP surface prevented NP uptake by vascular smooth muscle cells. Because macrophages are phagocytic and present at the aneurysmal site, we determined whether a negative surface charge would also prevent the uptake of NPs by macrophages. We showed that macrophages do not take up ~200 nm BB-94-loaded NPs (5:1 polymer to BB-94 ratio, negative surface charge). Based on these results and previous VSMC-uptake results, these NPs would remain in the ECM.

Elastin-antibody conjugation on the NP surface also allowed us to target these NPs to the site of elastin damage found in the aneurysm site because this antibody recognizes only core amorphous elastin that is exposed during elastic lamina degradation.[19] Our data with DIR dye-loaded NPs confirmed that they targeted only the injury site while sparing the healthy aorta. More importantly, we found that NPs entered preferentially from the adventitial side through the vasa vasorum and lodged deep in the media when delivered systemically. This is clinically advantageous because the intraluminal thrombus generally present in an aneurysm can obstruct NP-targeting from the luminal side. Notably, more degradation and inflammation are seen clinically in the adventitia.[27]

MMPs, in particular MMP-9 (gelatinase B/92 kDa) and MMP-2 (gelatinase A/72 kDa), play a significant role in AAA development and progression.[6] The goal of targeted treatment is to suppress MMP activity at the site of AAA so that further ECM degradation can be prevented. Our MMP fluorogenic assay showed that the MMP-2 and MMP-9 activity (represented as a ratio of abdominal aorta over thoracic aorta in the same animal) was 50% higher in the EL-NP-Blank and BB-94 IP groups, suggesting that sustained MMP activation was induced by $CaCl_2$ injury and was not inhibited in the abdominal aorta by these treatments. Only when BB-94 was delivered by targeted NPs (EL-NP-BB94) was a significant decrease in MMP activity seen in the abdominal aorta for prolonged periods, suggesting that targeted NPs delivered BB-94 at the site of injury and inhibited local MMP expression. This can either occur by the suppression of macrophage recruitment as we have

observed, which is consistent with previous study[28] or due to inhibition of MMPs secreted by VSMCs. These data are corroborated by the qualitative *in situ* zymography findings on histological sections of the abdominal aorta, which show suppression of gelatinolytic activity in tissues in the EL-NP-BB94 group alone.[29] Others have shown that a daily IP injection of 15 mg of BB-94 inhibited the expansion of AAA in elastase-induced aneurysms in rats.[15] However, the study lasted for only seven days, and AAA was treated only by the systemic inhibition of MMPs. We show that targeted NPs with very low concentrations of BB-94 injected only once weekly (equivalent to 25 μg total BB-94/animal/day) can significantly inhibit aneurysm expansion in a four week study. This corresponds to a 580-fold lower BB-94 concentration than others have used systemically.[15] Several clinical trials for systemic MMP inhibition as a cancer treatment failed because of poor bioavailability, dose limiting toxicity, and systemic side effects, such as musculoskeletal problems, that limited the dose that could be tolerated.[30] The side effects caused by MMP inhibitors in cancer patients led to the use of substantially lower doses of MMP inhibitors in clinical trials for aneurysm prevention.[31] The propranolol treatment was successful in aneurysm-prone turkeys and caused an increase in the tensile strength of tissue rings from the abdominal aorta.[32] However, clinical trials of the systemic delivery of, beta-blockers like propranolol, did not show significant changes in the growth rate of aneurysms, but caused systemic side effects and reduced patient compliance[33, 34], thus dampening enthusiasm for pharmacological therapy for AAA. Because our targeted treatment's site-specificity permits very low doses of the drug, such therapy would be an attractive option for preventing the expansion of aneurysms in patients without causing systemic side effects.

In conclusion, we demonstrate that targeted delivery of very small doses of MMP inhibitor BB-94 by NPs is an effective way to suppress MMP activity and aneurysmal development in an experimental rat model of AAA.

Supplementary Material

Refer to Web version on PubMed Central for supplementary material.

ACKNOWLEDGEMENT

We gratefully acknowledge funding from the NIH grant P20GM103444 and the Hunter Endowment at Clemson University to Naren Vyavahare. We would like to thank Jayesh Betala and Dr. Martine LaBerge for providing RASMCs.

Nonstandard Abbreviations and Acronyms

AAA	Abdominal aortic aneurysm
BB-94	Batimastat
DIR- 1	1-dioctadecyl-3, 3, 3, 3-tetramethylindotricarbocyanine iodide
ECM	Extracellular matrix
EL-NP-BB94	Elastin antibody conjugated BB-94 loaded nanoparticles
EL-NP-Blank	Elastin antibody conjugated blank nanoparticles

EL-NP-DIR	Elastin antibody conjugated DIR loaded nanoparticles
IgG-NP-DIR	IgG antibody conjugated DIR loaded nanoparticles
IP	Intraperitoneal injection
MMPs	Matrix metalloproteinases
NPs	Nanoparticles
PLA	Poly (D,L-lactide)
RASMC	Rat aortic smooth muscle cell
RAOEC	Rat aortic endothelial cells
TIMPs	Matrix metalloproteinases
VVG	Verhoeff-van Gieson

REFERENCES

1. Kuivaniemi H, Platsoucas C, Tilson MD III. Aortic aneurysms: An immune disease with a strong genetic component. Circulation. 2008; 117:242. [PubMed: 18195185]
2. Woessner, JF.; Nagase, H. introduction to Matrix metalloproteinases and timps. Oxford; New York: Oxford University Press; 2000. p. 1-10.
3. Morris DR, Biros E, Cronin O, Kuivaniemi H, Golledge J. The association of genetic variants of matrix metalloproteinases with abdominal aortic aneurysm: A systematic review and meta-analysis. Heart. 2014; 100:295–302. [PubMed: 23813847]
4. Sun J. Matrix metalloproteinases and tissue inhibitor of metalloproteinases are essential for the inflammatory response in cancer cells. Journal of Signal Transduction. 2010:1–7.
5. Raffetto JD, Khalil RA. Matrix metalloproteinases and their inhibitors in vascular remodeling and vascular disease. Biochemical pharmacology. 2008; 75:346–359. [PubMed: 17678629]
6. Thompson RW, Timothy B. MMP inhibition in abdominal aortic aneurysms: Rationale for a prospective randomized clinical trial. Annals of the New York Academy of Sciences. 1999; 878:159–178. [PubMed: 10415728]
7. Longo GM, Xiong W, Greiner TC, Zhao Y, Fiotti N, Baxter BT. Matrix metalloproteinases 2 and 9 work in concert to produce aortic aneurysms. The Journal of clinical investigation. 2002; 110:625–632. [PubMed: 12208863]
8. Kadoglou NP, Liapis CD. Matrix metalloproteinases: Contribution to pathogenesis, diagnosis, surveillance and treatment of abdominal aortic aneurysms. Current Medical Research and Opinion®. 2004; 20:419–432. [PubMed: 15119978]
9. Prescott MS, W K, Von Linden-Reed J, Jeune M, Chou M, Caplan SL, Jeng AY. Effect of matrix metalloproteinase inhibition on progression of atherosclerosis and aneurysm in ldl receptor-deficient mice overexpressing mmp-3, mmp-12, and mmp-13 and on restenosis in rats after balloon injury. Annals of the New York Academy of Sciences. 1999; 878:179–190. [PubMed: 10415729]
10. Brown PD. Matrix metalloproteinase inhibitors in the treatment of cancer. Medical Oncology. 1997; 14:1–10. [PubMed: 9232605]
11. Mannello F, Tonti G, Papa S. Matrix metalloproteinase inhibitors as anticancer therapeutics. Current Cancer Drug Targets. 2005; 5:285–298. [PubMed: 15975049]
12. Abbruzzese TA, Guzman RJ, Martin RL, Yee C, Zarins CK, Dalman RL. Matrix metalloproteinase inhibition limits arterial enlargements in a rodent arteriovenous fistula model. Surgery. 1998; 124:328–334. [PubMed: 9706156]
13. Erba E, Ronzoni S, Bassano L, Giavazzi R, D'Incalci M. The metalloproteinase inhibitor batimastat (bb-94) causes cell cycle phase perturbations in ovarian cancer cells. Annals of

oncology : official journal of the European Society for Medical Oncology / ESMO. 1999; 10:589–591. [PubMed: 10416010]

14. Moore G, Liao S, Curci JA, Starcher BC, Martin RL, Hendricks RT, Chen JJ. Suppression of experimental abdominal aortic aneurysms by systemic treatment with a hydroxamate-based matrix metalloproteinase inhibitor (rs 132908). Journal of vascular surgery. 1999; 29:522–532. [PubMed: 10069917]
15. Bigatel DA, Elmore JR, Carey DJ, Cizmeci-Smith G, Franklin DP, Youkey JR. The matrix metalloproteinase inhibitor bb-94 limits expansion of experimental abdominal aortic aneurysms. Journal of vascular surgery. 1999; 29:130–138. discussion 138–139. [PubMed: 9882797]
16. Epstein, CJ.; Erickson, RP.; Wynshaw-Boris, AJ. Inborn errors of development: The molecular basis of clinical disorders of morphogenesis. Oxford University Press; 2004. p. 977-980.
17. Sivaraman B, Ramamurthi A. Multifunctional nanoparticles for doxycycline delivery towards localized elastic matrix stabilization and regenerative repair. Acta biomaterialia. 2013; 9:6511–6525. [PubMed: 23376127]
18. Liu J, Xiong W, Baca-Regen L, Nagase H, Baxter BT. Mechanism of inhibition of matrix metalloproteinase-2 expression by doxycycline in human aortic smooth muscle cells. Journal of vascular surgery. 2003; 38:1376–1383. [PubMed: 14681644]
19. Sinha A, Shaporev A, Nosoudi N, Lei Y, Vertegel A, Lessner S, Vyavahare N. Nanoparticle targeting to diseased vasculature for imaging and therapy. Nanomed-Nanotechnol. 2014; 10:1003–1012.
20. Sinha A, Nosoudi N, Vyavahare N. Elasto-regenerative properties of polyphenols. Biochemical and Biophysical Research Communications Biochemical and Biophysical Research Communications. 2014; 444:205–211. [PubMed: 24440697]
21. Chronopoulou L, Massimi M, Giardi MF, Cametti C, Devirgiliis LC, Dentini M, Palocci C. Chitosan-coated plga nanoparticles: A sustained drug release strategy for cell cultures. COLSUB Colloids and Surfaces B: Biointerfaces. 2013; 103:310–317. [PubMed: 23261553]
22. Chiou AC, Chiu B, Pearce WH. Murine aortic aneurysm produced by periarterial application of calcium chloride. Journal of Surgical Research. 2001; 99:371–376. [PubMed: 11469913]
23. Kiliçarslan M, Baykara T. The effect of the drug/polymer ratio on the properties of the verapamil hcl loaded microspheres. International journal of pharmaceutics. 2003; 252:1–2. [PubMed: 12550776]
24. Botelho MA, Queiroz DB, Barros G, Guerreiro S, Fechine P, Umbelino S, Lyra A, Borges B, Freitas A, Queiroz DC, Ruela R, Almeida JG, Quintans L Jr. Nanostructured transdermal hormone replacement therapy for relieving menopausal symptoms: A confocal raman spectroscopy study. Clinics (Sao Paulo). 2014; 69:75–82. [PubMed: 24519196]
25. Patel PJ, Gohel MC, Acharya SR. Exploration of statistical experimental design to improve entrapment efficiency of acyclovir in poly (d, l) lactide nanoparticles. Pharmaceutical development and technology. 2014; 19:200–212. [PubMed: 23432525]
26. Sledge GWJ, Qulali M, Goulet R, Bone EA, Fife R. Effect of matrix metalloproteinase inhibitor batimastat on breast cancer regrowth and metastasis in athymic mice. Journal of the National Cancer Institute. 1995; 87:1546–1550. [PubMed: 7563189]
27. Houard X, Leclercq A, Fontaine V, Coutard M, Martin-Ventura J-L, Ho-Tin-Noé B, Touat Z, Meilhac O, Michel J-B. Retention and activation of blood-borne proteases in the arterial wallimplications for atherothrombosis. Journal of the American College of Cardiology. 2006; 48:A3–A9.
28. Bigatel DA, Elmore JR, Carey DJ, Cizmeci-Smith G, Franklin DP, Youkey JR. The matrix metalloproteinase inhibitor bb-94 limits expansion of experimental abdominal aortic aneurysms. Journal of vascular surgery. 1999; 29:130–139. [PubMed: 9882797]
29. Della PP, Soeltl R, Krell HW, Collins K, O'Donoghue M, Schmitt M, Krüger A. Combined treatment with serine protease inhibitor aprotinin and matrix metalloproteinase inhibitor batimastat (bb-94) does not prevent invasion of human esophageal and ovarian carcinoma cells in vivo. Anticancer research. 1998; 19:3809–3816.
30. Vandenbroucke RE, Libert C. Is there new hope for therapeutic matrix metalloproteinase inhibition? Nature Reviews Drug Discovery. 2014; 13:904–927. [PubMed: 25376097]

31. Fingleton B. Mmps as therapeutic targets—still a viable option? Seminars in cell & developmental biology. 2008; 19:61–68. [PubMed: 17693104]

32. Boucek RJ, Gunja-Smith Z, Noble NL, Simpson CF. Modulation by propranolol of the lysyl cross-links in aortic elastin and collagen of the aneurysm-prone turkey. Biochemical Pharmacology. 1983; 32:275–280. [PubMed: 6409122]

33. Mosorin M, Juvonen J, Biancari F, Satta J, Surcel H-M, Leinonen M, Saikku P, Juvonen T. Use of doxycycline to decrease the growth rate of abdominal aortic aneurysms: A randomized, double-blind, placebo-controlled pilot study. Journal of vascular surgery. 2001; 34:606–610. [PubMed: 11668312]

34. Investigators PAT. Propranolol for small abdominal aortic aneurysms: Results of a randomized trial. Journal of vascular surgery. 2002; 35:72–79. [PubMed: 11802135]

Novelty and Significance

What Is Known?

- No pharmacological treatments are currently available to halt abdominal aortic aneurysm (AAA) growth.
- Systemic drug therapies often have side effects.

What New Information Does This Article Contribute?

- Smart nanoparticles were designed to carry drugs to the AAA site.
- Systemic injection of nanoparticles led to delivery of the drug to the site of the aneurysm at very low drug doses, and the treatment inhibited aneurysmal growth.

AAA is an abnormal focal bulging of a vessel due to structural weakness. Currently there are few options to treat diagnosed AAA other than regular monitoring of its growth. Surgical placement of a vascular graft is not recommended until the diameter of the AAA reaches ~5 cm as the risk associated with the surgery outweighs the benefit; however, ten percent of deaths occur with AAA below that diameter. Systemic pharmacological treatments administered clinically to halt aneurysmal growth have not been successful. Matrix metalloproteinase-mediated elastic lamina degradation is the main cause of aneurysm formation, but global inhibition of MMPs is detrimental to healthy tissue.

We have developed a novel targeted, nanoparticle-based drug therapy for AAA. Using nanoparticles surface conjugated with an elastin antibody, which recognizes only degraded elastin, and loaded with an MMP inhibitor batimastat, we show that batimastat could be delivered to the site of the aneurysm in a calcium chloride injury model of AAA in rats. We found that nanoparticle injection inhibited AAA growth at a very low dose. Such targeted therapy could potentially be useful pharmacological therapy for treating patients with early stage AAA.

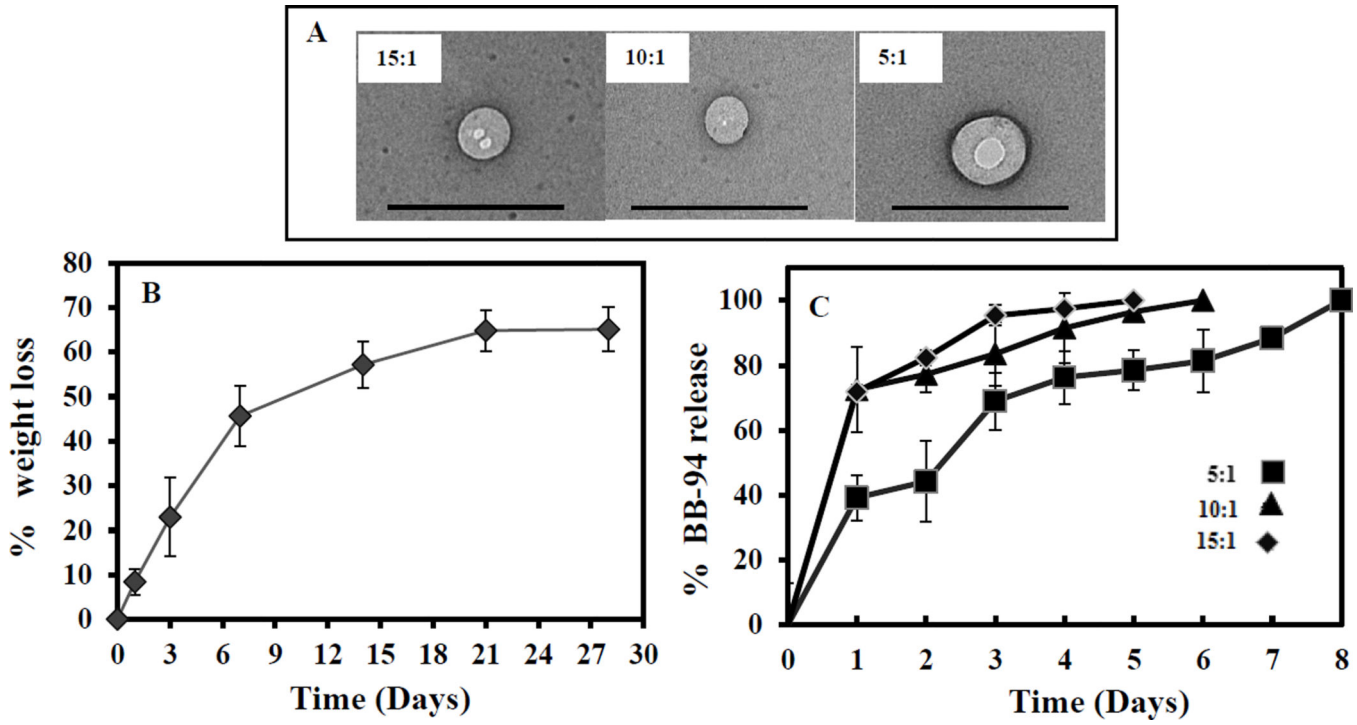

Figure 1. TEM, Degradation profile of NPs, and release of BB-94 from NPs

(A)TEM images of 15:1, 10:1, and 5:1 polymer to BB-94 ratio NPs. (B) Weight loss of blank NPs over four weeks. Weight loss showed the gradual polymeric degradation from Week 1 to Week 4. (n=3). (C) Release kinetics of BB-94 for 8 days. This 5:1 polymer to BB-94 ratio showed a more controlled and longer release profile (n=3).

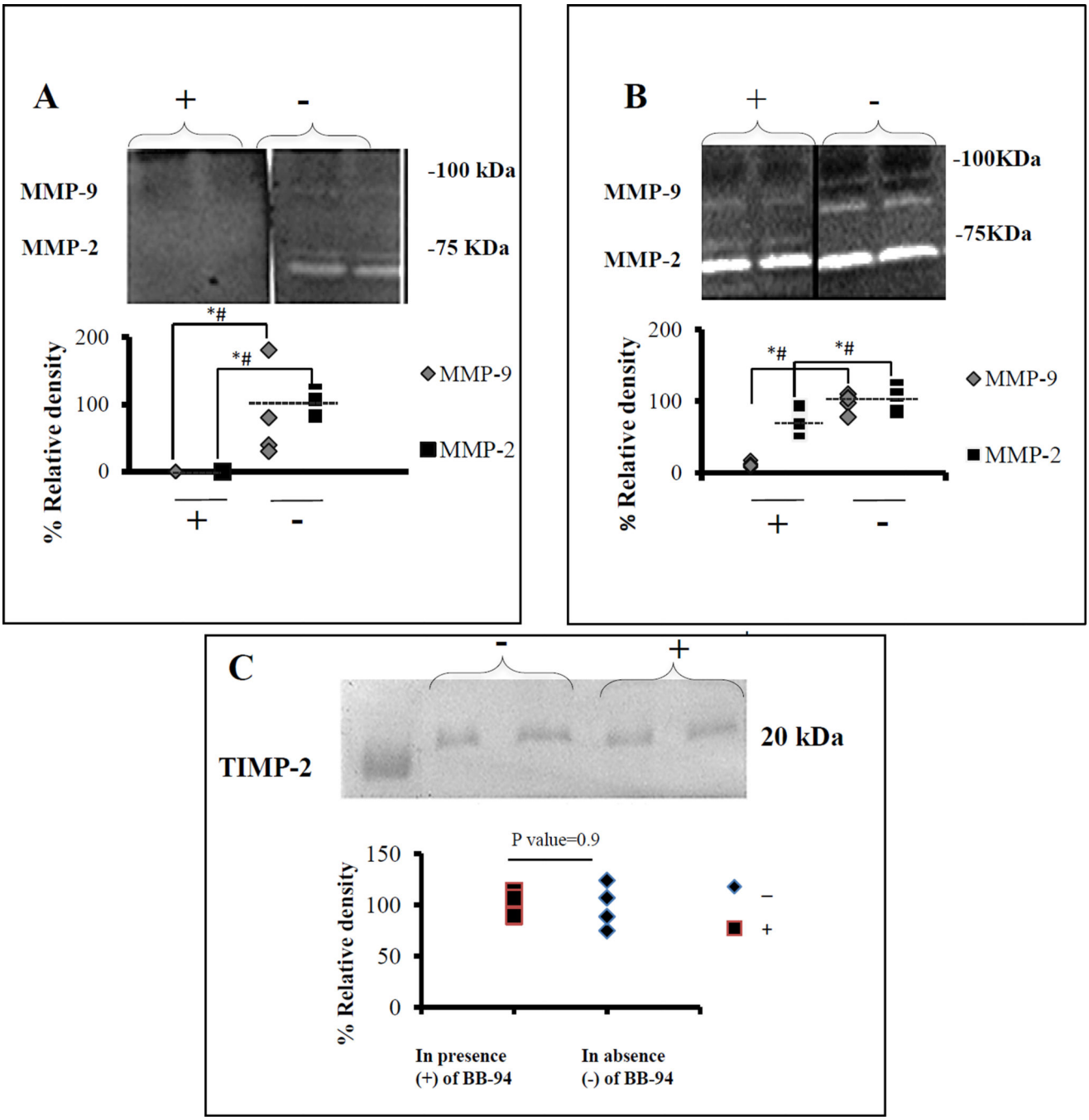

Figure 2. Activity of BB-94 in NPs

(A) Gel zymography study, BB-94 extracted from NPs was added to the development buffer (+), or no BB-94 (−). Relative activity of pro and active forms of MMP-2 and MMP-9 was totally inhibited by BB-94. (B) Cell-culture study, RASMCs treated with medium containing 500 nM extracted BB-94 in Dimethyl sulfoxide (+), RASMCs treated with Dimethyl sulfoxide alone (−). MMP-9 and active MMP-2 were inhibited 90% and 10%, respectively. (C) Reverse gel zymography showing no significant changes in TIMP-2 activity present in the cell culture medium of RASMCs either in the presence (+) or absence (−) of BB-94. *

(Student's unpaired *t* test, $P < 0.05$) and # (exact permutation test, $P < 0.05$). (n=6 for zymography and n=4 for reverse zymography). Dashed line represents the mean value.

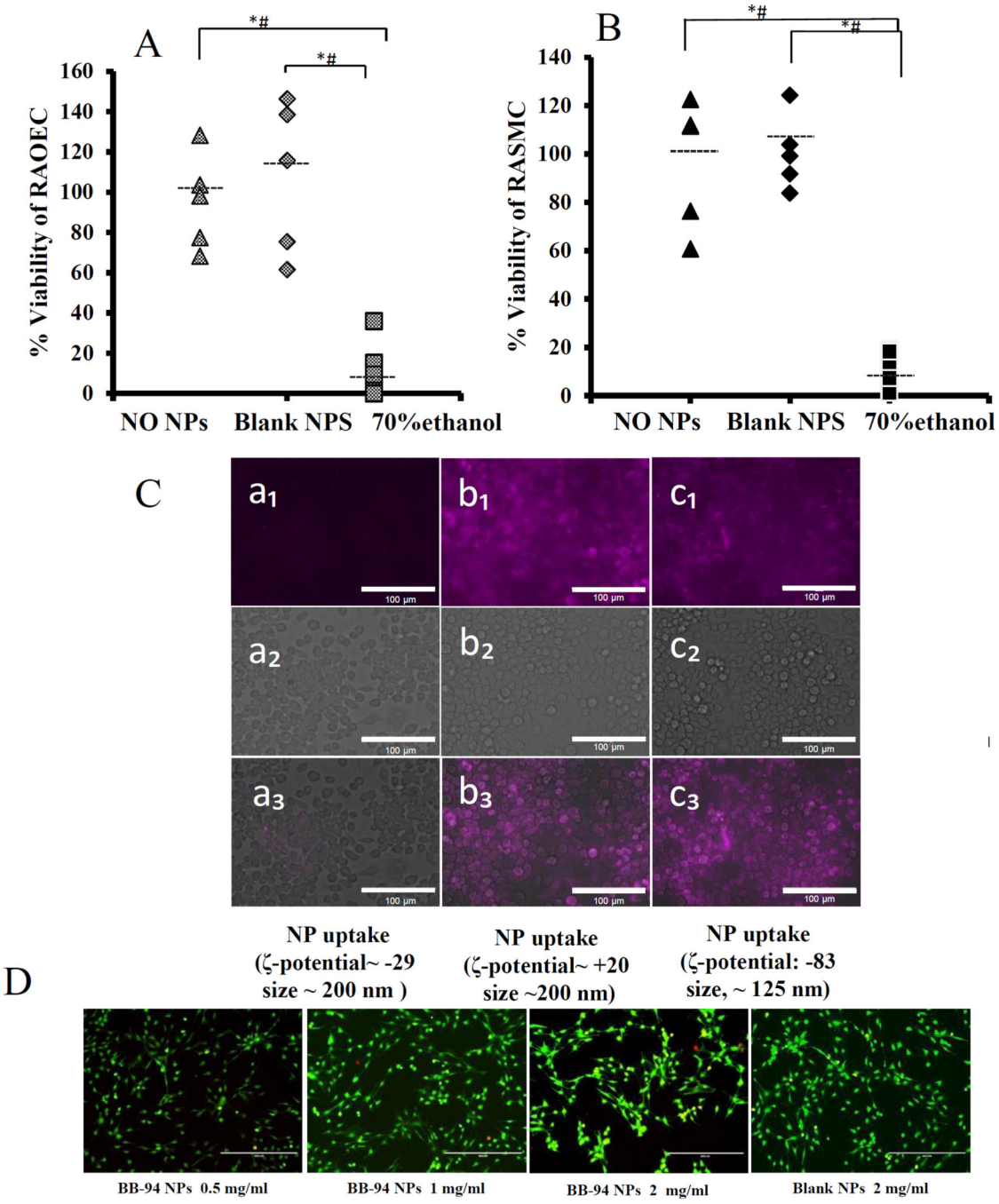

Figure 3. Macrophage uptake of elastin antibody conjugated NPs

(A) No change in RAOEC viability after incubation with blank NPs, 70% ethanol as positive control and no NPs as negative control(n=6) (B) No change in RASMC viability after incubation with blank NPs, 70% ethanol as positive control and no NPs as negative control(n=6). (C) DIR dye-loaded NPs (purple, size: 196 nm and ζ-potential: −29.1±5.1) after 24 hours incubation with macrophages showing no uptake (a_1 shows DIR loaded NPs, a_2 shows white light image and a_3 shows merged image). NPs were taken up by cells either when the surface charge was positive (b_1,b_2,b_3) or the size was small (c_1, c_2, c_3). Bar = 25

μM. (D) live/dead assay for macrophages incubated with BB-94-NPs for 24 hours; 0.5, 1, 2, and 2mg/ml Blank-NPs. None of the concentrations above showed any toxicity to the macrophages. * (Student's unpaired *t* test, $P < 0.05$) and # (exact permutation test, $P < 0.05$) (n=6). Dashed line represents the mean value.

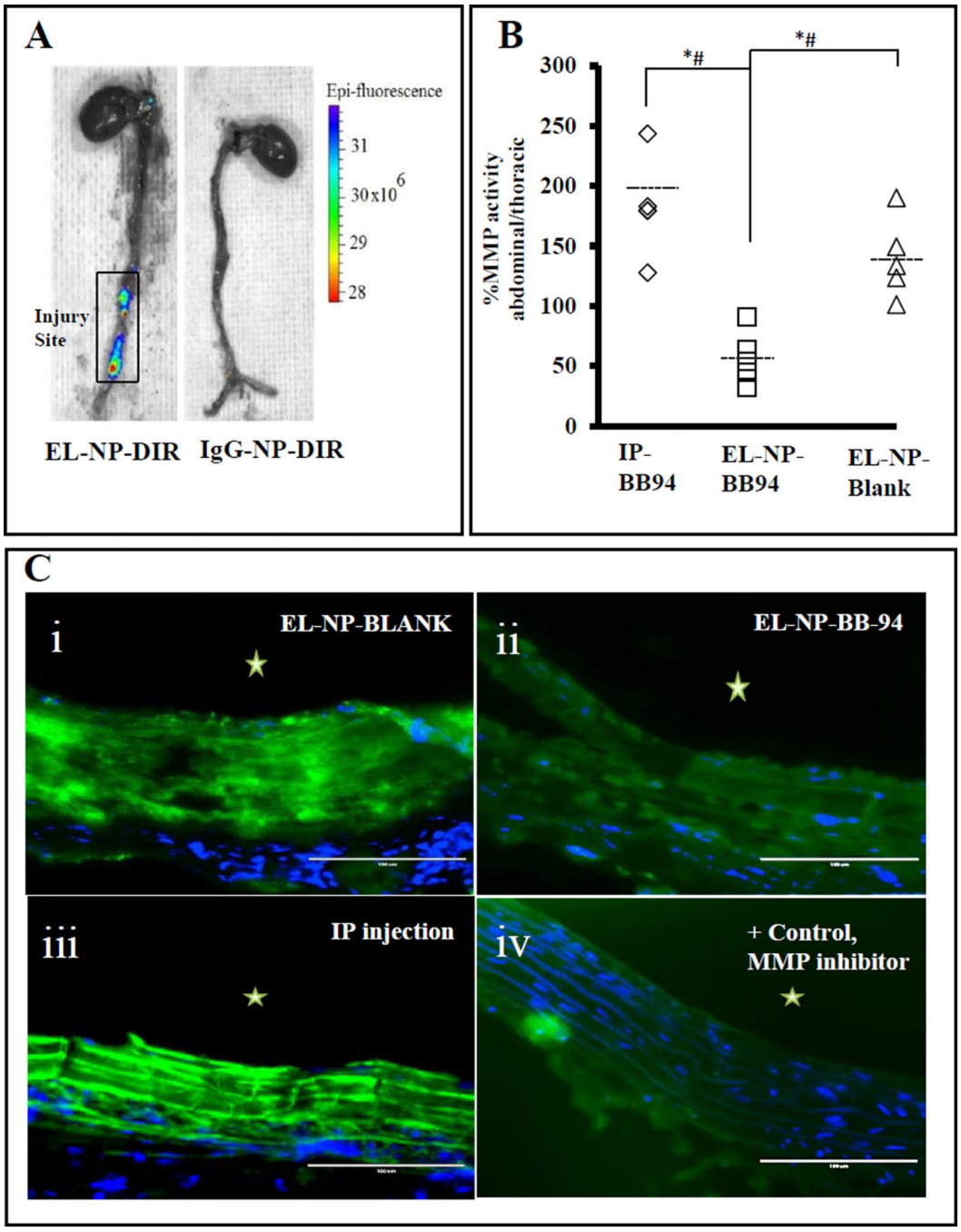

Figure 4. In vivo targeting of BB-94-loaded NPs

(A) Ten days after $CaCl_2$ injury, NPs were injected systemically (tail vein) and allowed to target for 48 hours. Fluorescent image of whole aorta taken by IVIS imaging system. Left: EL-NP-DIR group showing NPs targeting aneurysmal aorta while sparing healthy thoracic aorta, Right: IgG-NP-DIR group as control showing no targeting of NPs. (B) MMP activity as measured by fluorogenic substrate assay showing >150% increase in systemic BB-94 (at the same dose as BB-94 NPs, IP-BB94) and blank NP (EL-NP-Blank) groups in the abdominal aorta region ($CaCl_2$ mediated injury) compared to the thoracic aorta (non-injured,

healthy) showing MMPs were not inhibited in the abdominal aorta by these treatments. Only the EL-NP-BB94 group showed a significant decrease in MMP activity in the abdominal aorta. * (Student's unpaired *t* test, $P < 0.05$) and # (exact permutation test, $P < 0.05$) (n=5). Dashed line represents the mean value.

(C) Matrix metalloproteinase activity in abdominal aortic sections by *in situ* zymography. Green signal corresponds to active MMPs; blue signal corresponds to DAPI staining for cell nuclei. Only EL-NP-BB94 (ii) group shows suppression of MMPs while high MMP activity is seen in EL-NP-Blank (i) and IP-BB94 (iii). Positive control: abdominal aorta section incubated with MMP inhibitor shows minimal florescence (iv). * Indicates lumen. Bar = 100 μm.

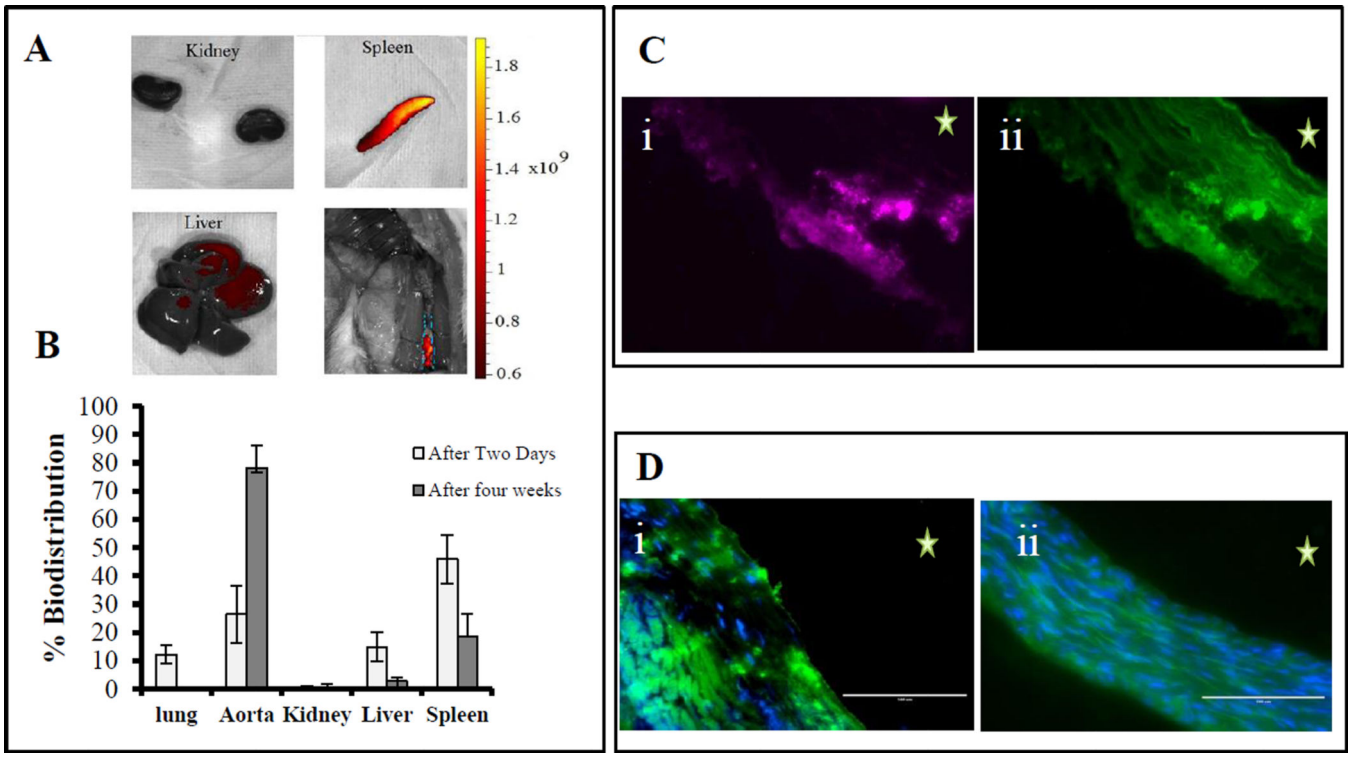

Figure 5. Long-term NP targeting

NPs accumulation after 4 weeks (once a week intravenous injection of EL-NP-DIR), (A) organ distribution of DIR NPs after four weeks; Fluorescent images of the kidney, spleen, liver and whole aorta were taken by IVIS imaging showing significantly higher fluorescence in the abdominal aorta in comparison to one injection,(B) Quantification of organ distribution after two days and four weeks, (C) Cross-section of abdominal aorta showing NPs (EL-NP-DIR) targeting from adventitial side and accumulation close to degraded elastic lamina; purple color for DIR fluorescence (i) matching with elastin degradation, green auto-fluorescence of elastin (ii); (D) Matrix metalloproteinase activity in abdominal aortic sections by *in situ* zymography at 38 days, green signal corresponds to active MMPs and blue signal to DAPI staining of cell nuclei. MMPs are very active in EL-NP-Blank group (i) while the EL-NP-BB94 (ii) group shows suppression of MMPs. * Indicates lumen. Bar = 100 μm.

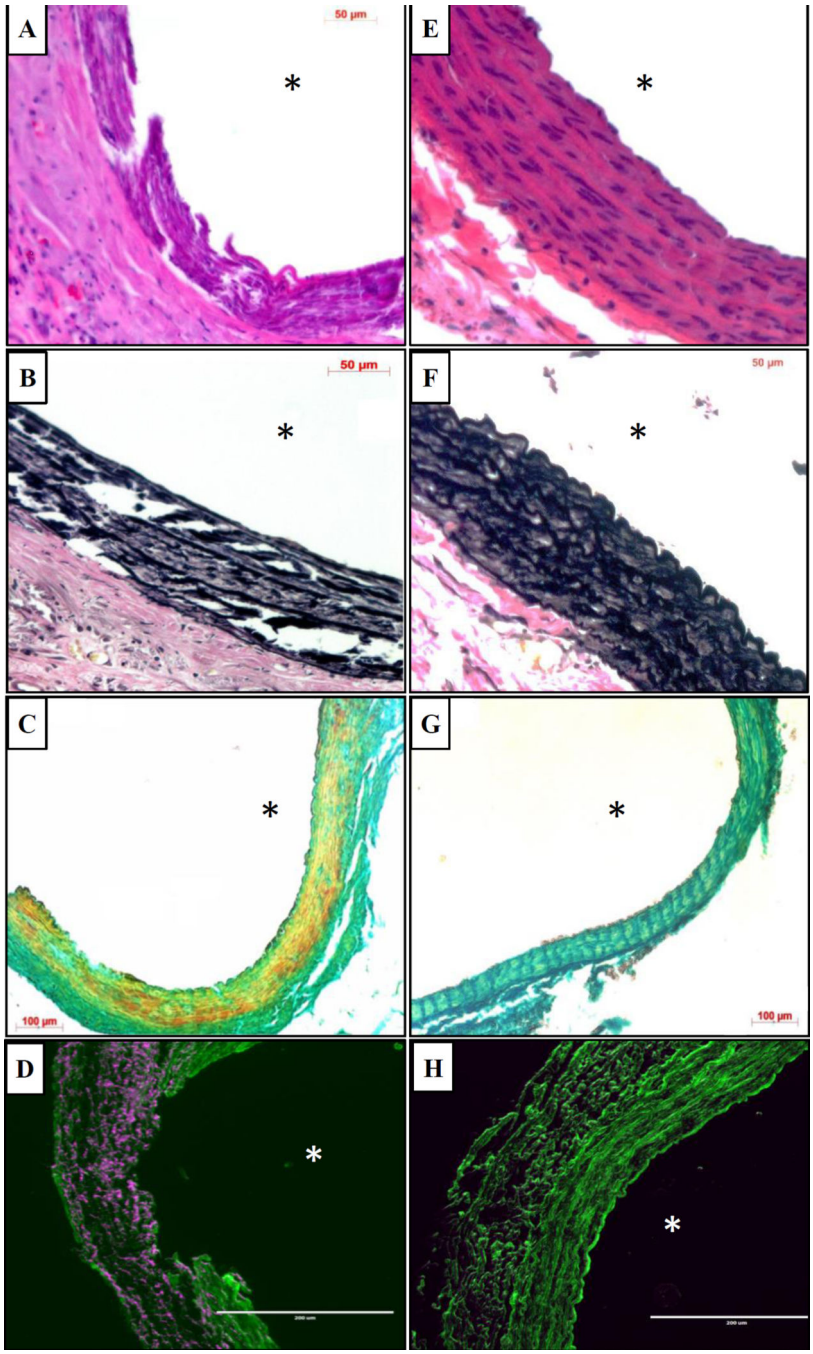

Figure 6. Histological analysis of abdominal aorta after 38 days

Hematoxylin and eosin staining (A and E) and VVG staining for elastin (B and F) of aortic sections showing medial elastic lamina damage in the EL-NP-Blank group with the presence of a significant adventitial inflammatory capsule while the media is intact in the EL-NP-BB94 group. Alizarin Red S staining for calcification (Red stain for calcium) with a Light Green SF counterstain (C and G) showing heavy calcification in the EL-NP-blank group while there is no calcification in EL-NP-BB94 treated group. Immunohistochemistry for M1 macrophages (purple color) showing high activity in the EL-NP-blank group while there is

very little macrophage activity in EL-NP-BB94 group (D and H).(A,B,C,D are EL-NP-blank group and E,F,G&H are EL-NP-BB94 group) * Indicates lumen.

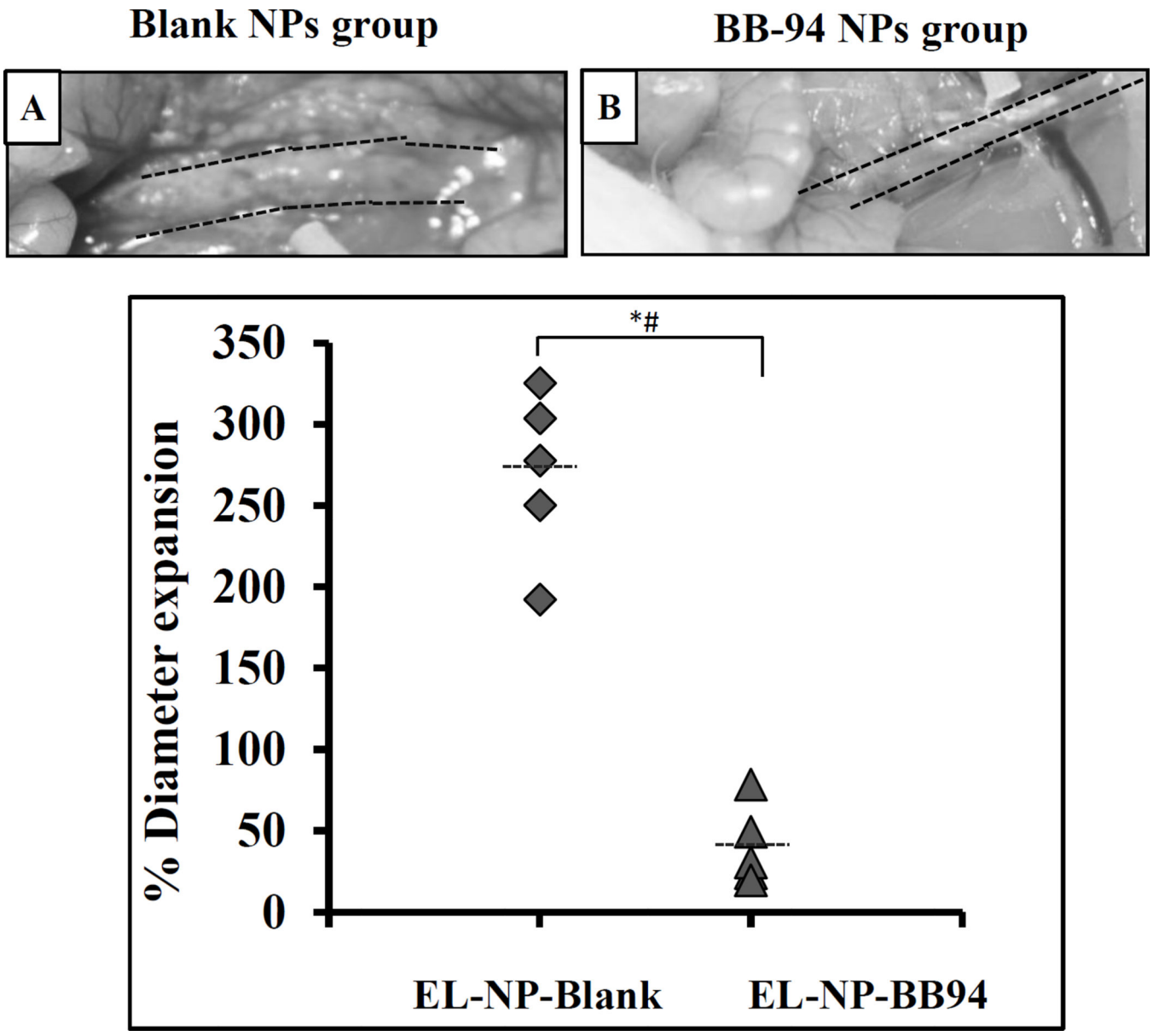

Figure 7. Inhibition of aneurysm development by targeted therapy

Targeted NPs with no drug (EL-NP-Blank) or with drug (EL-NP-BB94) were intravenously administered once a week for four weeks. Aneurysmal development in the blank NP group was significantly higher in comparison to the group receiving BB-94 NPs. * (Student's unpaired *t* test, $P < 0.05$) and # (exact permutation test, $P < 0.05$). (A and B) representative images of aorta at sacrifice, (C) external diameter in two groups (n=5).

TABLE 1

Characterization of nanoparticles and BB-94 loading

Polymer / BB- 94 ratio	% Yield n=4	% Loading n=3	NP size (nm) n=3	ζ-potential (mV) n=3
15:1	62.9± 33.9	5.7 ± 2.5	123.8 ± 24.9$^{\#}$	−83.1 ±2.8$^{\#*}$
10:1	44.2 ± 3	8.4 ± 2.7	153.5 ± 26.8$^{\#}$	−47.2±5.5$^{\#*}$
5:1	38.4 ± 18	6.7 ± 0.4	196.3 ± 3.3	−29.1±5.1

*represents statistical significance (Student's unpaired t-test, $P < 0.05$),

$^{\#}$represents statistical significance (exact permutation test, $P < 0.05$) compared to 5:1 group.